# SPE 130343

# Non-Darcy Displacement in Linear Composite and Radial Flow Porous Media

Yu-Shu Wu, Perapon Fakcharoenphol, and Ronglei Zhang, Colorado School of Mines



This paper was prepared for presentation at the SPE EUROPEC/EAGE Annual Conference and Exhibition held in Barcelona, Spain, 14–17 June 2010.



## Abstract

This paper presents Buckley-Leverett type analytical solutions for non-Darcy displacement of two immiscible fluids in linear and radial composite porous media. High velocity or non-Darcy flow commonly occurs in the vicinity of wellbore because of smaller flowing cross-sectional area, however, the effect of such non-Darcy has been traditionally ignored. To examine physical behavior of multiphase immiscible fluid non-Darcy displacement, an extended Buckley-Leverett type of solution is discussed.

There exists a Buckley-Leverett type solution for describing non-Darcy displacement in a linear homogeneous reservoir. This work extends the solution to flow in linear and radial composite flow systems. We present several new Buckley-Leverett type analytical solutions for non-Darcy flow in more complicated flow geometry of linear and radial composite reservoirs, based on non-Darcy flow models of Forchheimer and Barree-Conway. As application examples, we use the analytical solutions to verify numerical simulation results as well as to discuss non-Darcy displacement behavior. The results show how non-Darcy displacement in linear and radial composite systems are controlled not only by relative permeability, but also non-Darcy coefficients, characteristic length, injection rates, and as well as discontinuities in saturation profile across the interfaces between adjacent flow domains.

## Introduction

Multiphase flow and displacement occurs in a large variety of subsurface systems ranging from gas, oil, and geothermal reservoirs, vadose zone hydrology, and soil sciences. In oil and gas industry, fluid displacement has long been used as an effective EOR process. Buckley and Leverett [1942] established the fundamental principle for flow and displacement of immiscible fluids through porous media in their classic study of fractional flow theory. Their solution involves the displacement process of two incompressible, immiscible fluids in a one-dimensional, homogeneous system without considering capillary effect. The solution, then, has been extended in many aspects e.g. including capillary effects [Yortsos and Fokas, 1983; Chen, 1988; Mc-Whorter and Sunada, 1990], heterogeneous reservoir, linear composite,Wu [1993].

The effects of non-Darcy or high-velocity flow regimes in porous media have long been noticed and investigated for porous media flow (e.g., Tek et al., 1962; Scheidegger, 1972; Katzand Lee, 1990;Wu, 2002).

Theoretical, field, and experimental studies performed on non-Darcy flow in porous media both on singlephase [Tek et al., 1962; Swift and Kiel, 1962; Lee et al., 1987] and multiphase flow [Lai et al 2009]. Clasical non-Darcy flow is described using Forchheimer equation for a singlephase system. Many studies [e.g., Evans and Evans, 1988; Liu et al., 1995; Wu et al., 2002] extended the equation to multiphase flow. Recent studies [Baree and Conway, 2004, 2007] have indicated that Forchheimer equation could not accurately predict fluid flow behavior in porous media at very high velocity. As such, an alternative correlation in both singlephase and multiphase flows was presented. Laboratory studies [Lai et al, 2009] confirmed this, Baree-Conway, model. However, as Forchheimer are still in use widely, in this work, both non-Darcy equations are used.

This paper presents a Buckley-Leverett analytical solution for one-dimension non-Darcy displacement of two-phase immiscible fluids in linear and radial composite porous media. The classical Buckley-Leverett principle is used as well as non-Darcy flow in a heterogeneous porous media, in which the two-phase fluids conform to non-Darcy displacement and the formation is treated as consisting of two flow domains with different rock property. A practical procedure for calculate the wetting phase saturation profile for non-Darcy immiscible displacement in one-dimension linear and radial composite system is provided. The analytical solution and the resulting procedure can be regarded as an extension of the Buckley-Leverett theory.

## Mathematical Model

Consider the flow of two immiscible fluids (one wetting and one nonwetting phase) in a homogeneous, isothermal, and isotropic porous medium. Assume that no interphase mass transfer occurs between the two fluids and ignore dispersion and adsorption effects. The governing equation for fluid $f$ is given by the mass conservation equation,

$$-\nabla\cdot\left(\rho_f v_f\right)+q_f=\frac{\partial}{\partial t}\left(\rho_f S_f \phi\right) \tag{1}$$

where, $f$ is fluid ($f=w$ for the wetting phase and $f=n$ for the nonwetting phase), $\rho$ is the density of fluid, $v$ is the volume matrix (or Darcy flow) velocity, $q$ is sink/source term, $S$ is the saturation, $t$ is time, and $\phi$ is the effective porosity of formation

To incorporate non-Darcy flow behavior, volume matrix velocity ($v_f$) is treated using non-Darcy flow equations. In this study, two equations are of interest. First, the Forchheimer non-Darcy flow equation.

$$-\nabla\Phi_f=\frac{\mu_f}{kk_{rf}}v_f+\beta_f\rho_f v_f\left|v_f\right| \tag{2}$$

where, $v_f$ is volume matrix (Darcy) velocity, $\Phi$ is flow potential, $k$ is the absolute permeability of the porous media, $g$ is the gravitational constant, $k_{rf}$ is the relative permeability to fluid $f$, $\mu_f$ is the dynamic viscosity of fluid $f$, and $\beta_f$ is the effective non-Darcy flow coefficient (per meter) for fluid $f$ under multiphase flow conditions described as follows [Evans and Evans, 1988].

$$\beta_f=\frac{C_\beta}{\left(kk_{rf}\right)^{5/4}\left[\phi\left(S_f-S_{fr}\right)\right]^{3/4}} \tag{3}$$

where $C_\beta$ is a non-Darcy flow constant with a unit of meters$^{3/2}$ if converted to SI units. A recent study [Liu et

al., 1995] indicates that the $\beta$ coefficient may be also correlated to tortuosity or the representative length of tortuous flow paths in pore structure of a porous media. According to Wu [2002], volume matrix velocity can be computed in a simplified form for a constant cross-sectional area as follows:

$$v_f = \frac{1}{2k\rho_f\beta_f}\left[-\frac{\mu_f}{k_{rf}} + \left(\frac{\mu_f}{k_{rf}}\right)^2 - 4k^2\rho_f\beta_f\left(\frac{\partial\Phi_f}{\partial x}\right)\right]^{1/2} \tag{4}$$

Recent studies [Baree and Conway, 2004, 2007] indicated that Forchheimer equation could not accurately predict fluid flow behavior in porous media at very high velocity and presented an alternative equation in both singlephase and multiphase flows.

$$-\nabla\Phi_f = \frac{\mu_f v_f}{k_d k_{rf}\left(k_{mr} + \dfrac{(1-k_{mr})\mu_f\tau}{\mu_f\tau + \rho_f\left|v_f\right|}\right)} \tag{5}$$

where $k_d$ is absolute (Darcy) permeability, $k_{mr}$ is the minimum permeability ratio at high rate, relative to absolute (Darcy) permeability, $\tau$ is the characteristic length.

Wu [2009] proposed the method to include Baree-Conway model into numerical simulation and Buckley-Leverett analytical typw of solutions.the simplified from of volume matrix velocity of Baree and Conway non-Darcy flow for a constant cross-sectional area as follows [Lai, 2009]:

$$v_f = \frac{-a_1 + \sqrt{a_1^2 - 2\mu_f\rho_f k_d k_{rf} k_{rm}\mu_\beta S_\beta\tau\dfrac{\partial\Phi_f}{\partial x}}}{2\mu_f\rho_f} \tag{6}$$

where $a_1 = \mu_\beta^2 S_\beta\tau + k_d k_{rf} k_{rm}\rho_f\dfrac{\partial\Phi_f}{\partial x}$ ,

Equation (4) and (6) implicitly defines the volume matrix velocity as a function of pressure gradient as well as saturation, relative permeability, effective non-Darcy flow coefficient, minimum permeability ratio, and characteristic length. A more general relation for the Darcy velocity in multiphase non-Darcy flow may be proposed as follows:

$$v_f = v_f\left(\nabla\Phi_f, S_f\right) \tag{7}$$

## Analytical Solution for One-Dimension Linear and Radial Systems

The classical Buckley-Leverett solution was derived assuming the following flow conditions. (1) Both fluids and the porous medium are incompressible. (2) Capillary pressure gradient is negligible. (3) Gravity segregation effect is negligible (i.e., stable displacement exists near the displacement front).

For a one-dimension flow and displacement in a linear system, a semi-infinite linear flow system with a

constant cross-sectional area ($A$), Equation (1) can be rewritten as follows:

$$\frac{\partial x_s}{\partial t} = \frac{q_i}{\phi A}\left(\frac{\partial f_f}{\partial S_f}\right)_s \tag{8}$$

where, $x_s$ is the location of tracking saturation along x-direction, $q_i$ is injection rate, $A$ is cross-sectional area, $f_f$ is fractional flow of fluid $f$, $S_f$ is saturation of fluid $f$

Using the same assumptions, the mass conservation of a one-dimension flow and displacement in a radial system can be rewritten as follows:

$$\frac{\partial r_s^2}{\partial t} = \frac{q_i}{\phi \pi h}\left(\frac{\partial f_f}{\partial S_f}\right)_s \tag{9}$$

where, $r_s$ is the location of tracking saturation away from the injecting point, h is reservoir thickness

To complete the mathematical description of the physical problem, the initial and boundary conditions must be specified. The system is initially assumed to be uniformly saturated with both wetting and nonwetting fluids. The wetting phase is at its residual saturation, and a nonwetting fluid, such as oil or gas, is at its maximum saturation in the system as follows:

$$S_n(x/r, t = 0) = 1 - S_{wr} \tag{10}$$

where $S_{wr}$ is the initial, residual wetting phase saturation. Wetting fluid, such as water, is continuously being injected at a known rate $q_i(t)$, generally a function of injection time ($t$). Therefore the boundary conditions at the inlet are

for a linear system

$$v_w(x = 0, t) = \frac{q_i(t)}{A} \tag{11}$$

$$v_n(x = 0, t) = 0 \tag{12}$$

for a radial system

$$v_w(r = r_w, t) = \frac{q_i(t)}{2\pi r_w h} \tag{13}$$

$$v_n(r = r_w, t) = 0 \tag{14}$$

The fractional flow of a fluid phase is defined as a volume fraction of the phase flowing at a given location and time to the total volume of the flowing phases [Willhite, 1986]. The fractional flow can be written as

$$f_f = \frac{v_f}{v_w + v_n} = \frac{v_f}{v_t(t)} \tag{15}$$

From volume balance due to incompressibility of the system we have

$$f_w + f_n = 1 \tag{16}$$

## Solution Procedure

The general solution procedure is shown in Fig. 1. This procedure applies for both linear and radial composite systems as well as for Forchheimer and Baree-Conway non-Darcy models.

1. In order to calculate saturation profile in such complex systems, we have to discretize flow domain into series of homogeneous with a constant total volume matrix velocity ($v_t$).

2. Calculate total volume matrix velocity ($v_t$) from the following equations:

$$v_t = \frac{q_i(t)}{A} \tag{17}$$

   where $A$ is a constant cross-sectional area for a linear composite and $A = 2\pi rh$ for a radial composite

3. Calculate potential gradient profile: from Equation (3), (4), and (5), fluid velocity is a function of potential gradient ($\nabla\Phi_f$) and phase saturation ($S_f$).As no capillary pressure is assumed for a water-oil system, oil potential and water potential are the same. Using the fact that a total velocity is constant for a particular segment, we can setup Equation (16) and use Newton's Iteration method to solve for a potential gradient for a given saturation

$$v_t - v_w(\nabla\Phi_w, S_w) - v_n(\nabla\Phi_n, 1 - S_w) = 0 \tag{18}$$

4. Calculate fractional flow: for each segment, a fractional flow curve can be computed from Equation (15)

5. Select any tracked saturation: this apparent saturation in the first segment is used to track its location and the apparent saturation in other segments after injection for a given time. Using the continuity condition for interface of each segment , an apparent saturation can be determined as follows

$$f_{w1}(S_{w1}) = f_{wm}(S_{wm}) \tag{19}$$

   where, $m$ is any segment number

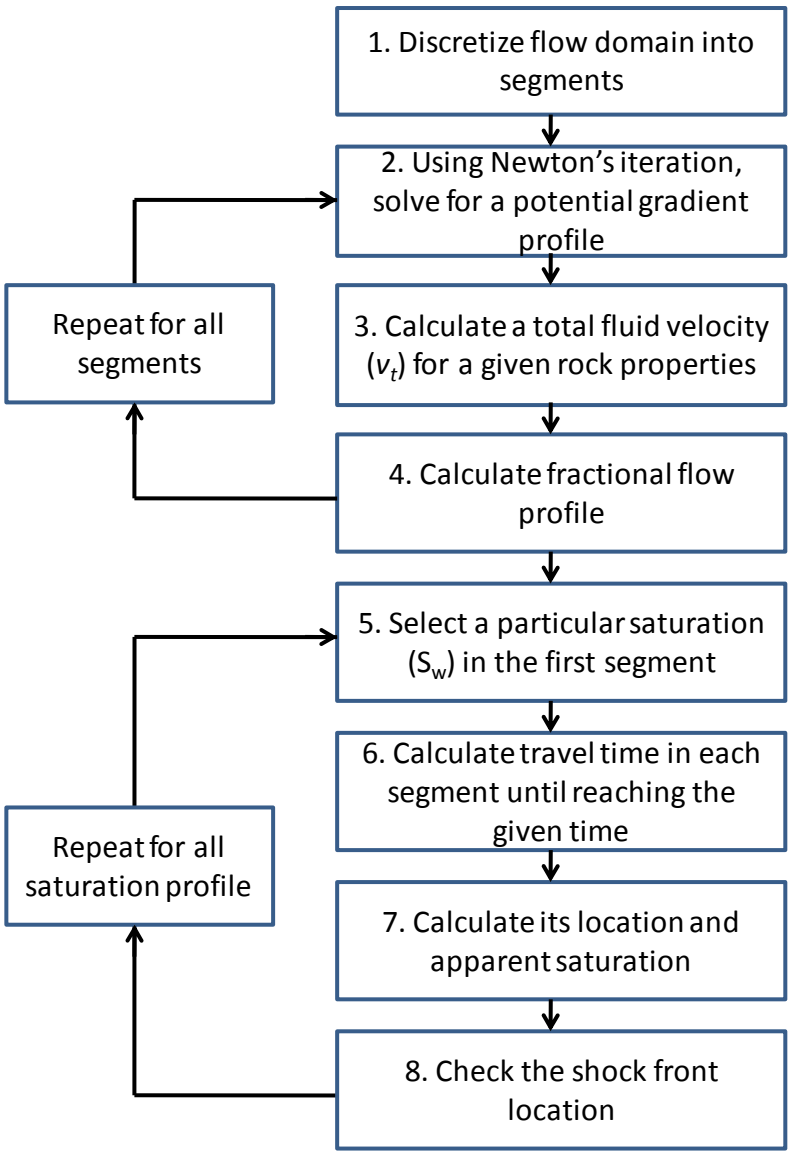


Fig. 1 Solution Procedure Diagram

6. Compute the travel time in each segment as follows, see Appendix A for example of calculation:

$$\Delta t_j = \frac{\phi_j A}{q_i}\left(\frac{\partial f_w}{\partial s_w}\right)_{S_j}^{-1} \Delta x_j \qquad \text{for a linear composite}$$

$$\Delta t_j = \frac{(\phi \pi h)_j}{q_i}\left(\frac{\partial f_w}{\partial s_w}\right)_{S_j}^{-1} r_j^2 \qquad \text{for a radial composite} \qquad (20)$$

where, $S_j$ is an apparent saturation in segment $j$

Then check segment number that the selected saturation locates for a given time

$$\sum_{j=1}^{m-1}\Delta t_j < t < \sum_{j=1}^{m}\Delta t_j \qquad (21$$

where, $m$ is the segment number that the selected saturation locate

7. Calculate the location of the saturation:

$$x_s = \sum_{j=1}^{m-1}\Delta x_j + \frac{q_i}{\phi_m A}\left(\frac{\partial f_w}{\partial S_w}\right)_{S_m}\left(t - \sum_{j=1}^{m-1}\Delta t_j\right) \qquad \text{for a linear composite}$$

$$r_s^2 = \sum_{j=1}^{m-1}\Delta r_j^2 + \frac{q_i}{\phi_m \pi h}\left(\frac{\partial f_w}{\partial S_w}\right)_{S_m}\left(t - \sum_{j=1}^{m-1}\Delta t_j\right) \qquad \text{for a radial composite} \qquad (22)$$

where. $x_s$ and $r_s$ are location of the saturation, $S_m$ is an apparent saturation in segment $m$

8. Check the shock front location: we can use total amount of injection volume to check saturation of the shock front as follows

$$q_i t - \phi A\int_0^{x_s}\left(S_w - S_{wr}\right)dx \le 0 \qquad \text{for a linear composite}$$

$$q_i t - \phi \pi h\int_{r_w}^{r_s}\left(S_w - S_{wr}\right)dr^2 \le 0 \qquad \text{for a radial composite} \qquad (23)$$

If the condition hold, the calculated saturation is belong to the shock front

## Discussions

The extension Buckley-Leverett solution described above is used to demonstrate influences of input parameters, e.g. injection rate, non-Darcy coefficient in Forchheimer correlation, characteristic length and minimum permeability ratio in Barree-Conway correlation, on water saturation profile as well as displacement efficiency. One-dimension linear-composite, where porosity, permeability of rocks are the same for both rocks, only relative permeability are different, see Table 1, models are setup with the same initial condition. Water saturation distributes uniformly at the irreducible water saturation ($S_{wr}$=0.2) and water is injected with a constant volumetric rate at inlet (x=0).

Fig.2-4 illustrate base case scenario where the operating condition and time are given in Table 1. Water saturation discontinuity appears at the rock interface due to change in rock properties. Fig 5-8 show the sensitivity of input parameters for both Forchheimer and Baree-Conway correlations. These input parameters control fractional flow curve and, as the results, control water saturation profile and displacement efficiency.

One important thing is that non-Darcy phenomena improves displacement efficiency because any saturation moving with high velocity is held back by non-Darcy effect. Consequently, saturation profile moves in a more-uniform manner, see the injection rate sensitivity Fig 7.

For sensitivity cases of Baree-Conway non-Darcyequation, Equation (5), if the characteristic length ($\tau$) goes to infinity, the equation can be reduced to the standard Darcy's equation as such the higher the characteristic length, the less the non-Darcy effect is. This effect can be seen in Fig 5. High characteristic length or high non-Darcy effect reduces the shock front speed and uniform saturation front. In the minimum permeability ratio case, the ratio value ranges from zero to one. According to Equation (5) if the ratio approaches one, the equation is in the same form as Darcy described. A small minimum permeability ratio physically means that it is the smallest equivalent Darcy permeability possible of non-Darcy system can be. As such the smaller the ratio, the more the non-Darcy effects is, this effect is observed here in Fig 6.

## Application Example

One application of this extended Buckley-Leverett solution is to use as a verification tools for numerical simulation development. In this case, MSFLOW code [Wu, 1998], a general purpose, three-phase reservoir simulator, is verified with the solution. Two one-dimensional reservoir systems are modeled for linear and radial composite. To reduce the effects of discretization on numerical simulation results, very fine, uniform mesh spacing ($\Delta x$ = 0.01 m and $\Delta r$ = 0.01 m) are chosen. The flow description and the parameters for this problem are identical to those in Table 1 for the case of characteristic length is 1000 and Minimum Permeability ratio is 0.01.

The comparisons between the analytical and numerical solutions for linear and radial composite are shown in Fig 10 and 12, respectively. Both indicate that the numerical results are in excellent agreement with the analytical prediction of the non-Darcy displacement for the entire wetting phase sweeping zone. Except at the shock, advancing saturation front, the numerical solution deviates only slightly from the analytical solution, resulting from a typical "smearing front" phenomenon of numerical dispersion effects when matching the Buckley-Leverett solution using numerical results [Aziz and Settari, 1979].

## Conclusions

This paper presents a Buckley-Leverett analytical solution and a theoretical study for non-Darcy displacement of two immiscible fluids through linear and radial composite porous media. A general procedure is developed to solve such a complex reservoir system analytically. This procedure can be used for any non-Darcy equation.

In this work, non-Darcy effect is treated using Forchheimer and Baree-Conway equations. Effects of variation of physical parameters for each non-Darcy equation are run to investigate how these parameters influence water saturation profile as well as displacement efficiency. The results show that non-Darcy displacement in linear and radial composite systems are controlled not only by relative permeability, but also non-Darcy coefficients, characteristic length, injection rates, and as well as discontinuities in saturation profile across the interfaces between adjacent flow domains. One important thing to emphasize here is that non-Darcy effect help improve displacement efficiency because any saturation moving with high velocity is held back by non-Darcy effect. Consequently, saturation profile moves in a more-uniform manner. As an example of application, the analytical solution is applied to verify a numerical simulator modeling multiphase non-Darcy flow.

| General Information | Linear Composite |
|---|---|
| Cross section Area(m^2) | 1.00E+00 |
| Time (s) | 4.00E+04 |
| Rate (m^3/s) | 1.00E-05 |
| Nondarcy Option | Baree-Conway |

| Rock Properties | Rock 1 | Rock 2 |
|---|---|---|
| Permeability, $m^2$ | 1.00E-13 | 1.00E-13 |
| Length, m | 2.0 | 4.0 |
| Porosity, fraction | 0.3 | 0.3 |
| Relative Permeability to Water,fraction | $0.75(Sw-0.2)^{2.5}$ | $0.5(0.8-Sw)^{1.5}$ |
| Relative Permeability to Oil, fraction | $0.25(Sw-0.2)^{1.5}$ | $0.5(0.8-Sw)^{2.5}$ |
| Minimum Permeability Relative to Darcy's Permeability, fraction | 1.00E-02 | 1.00E-02 |
| Characteristic lenght, m/10000 | 1.00E+03 | 1.00E+03 |

| Fluid Properties | Water | Oil |
|---|---|---|
| Viscosoty, Pa.s | 1.00E-03 | 5.00E-03 |
| Density, $kg/m^3$ | 1.00E+03 | 8.00E+02 |

Table 1 Parameter for Non-Darcy Barree-Conway Immiscible Displacement in a Linear Composite System

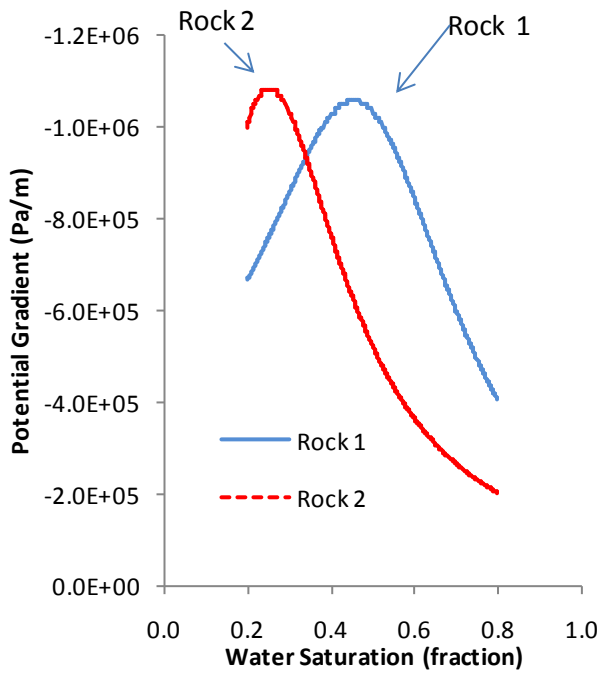


Fig. 2 Potential Gradient Profile

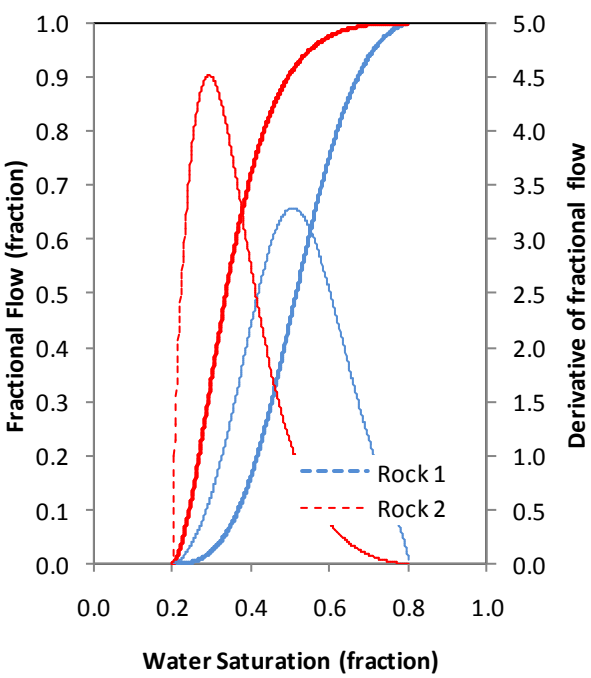


Fig. 3 Fractional Flow and Its Derivative

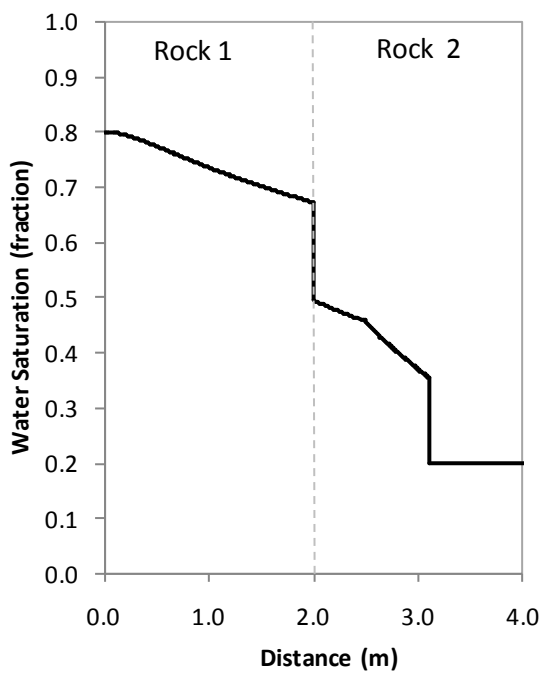


Fig. 4 Saturation Profile

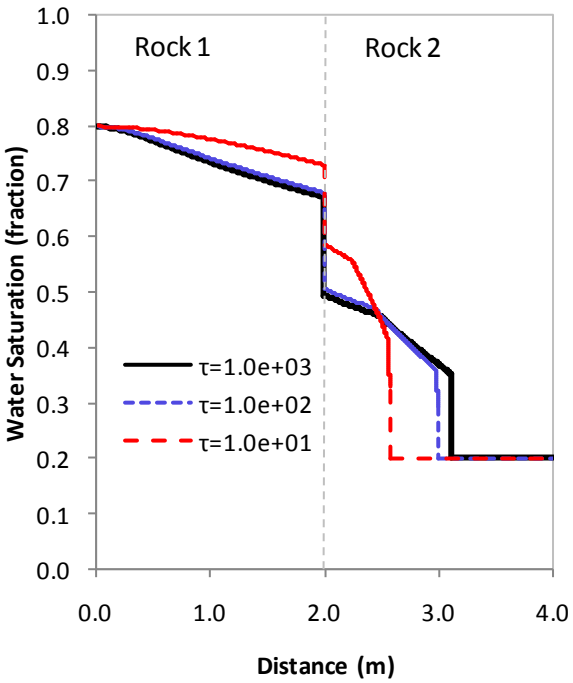


Fig. 5 Saturation Profile
Comparing characteristic length Sensitivity

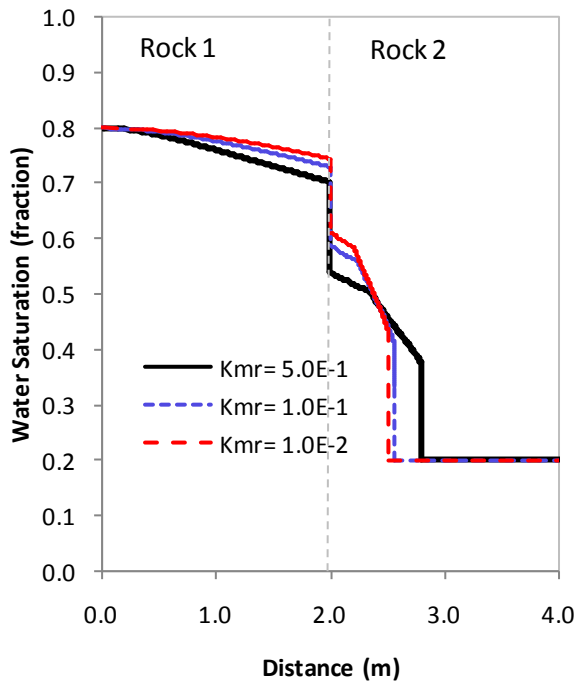


Fig. 6 Saturation Profile Comparing
Minimum Permeability ratio Sensitivity

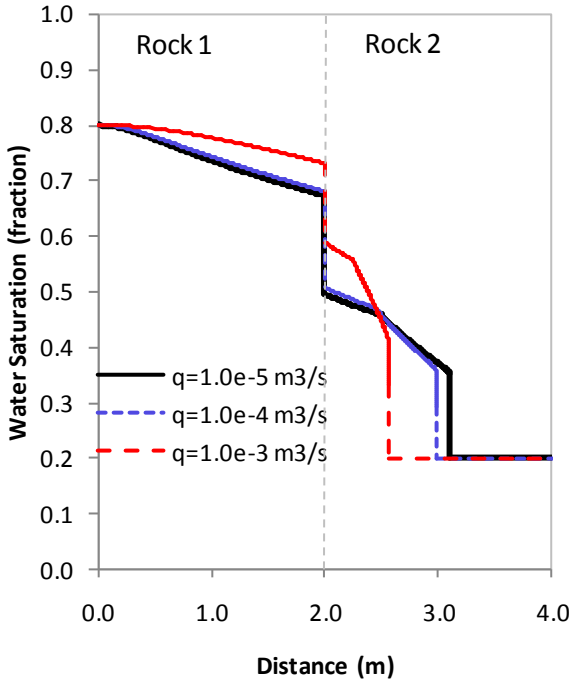


Fig. 7 Saturation Profile
Comparing Injection Rate Sensitivity

| General Information | Linear Composite | |
|---|---|---|
| Cross section Area, $m^2$ | 1.00 | |
| Time (s) | 4.00E+04 | |
| Rate (m^3/s) | 1.00E-05 | |
| Nondarcy Option | Forchheimer | |
| | | |
| Rock Properties | Rock 1 | Rock 2 |
| Permeability, $m^2$ | 1.00E-13 | 1.00E-13 |
| Length, m | 2.0 | 2.0 |
| Porosity, fraction | 0.3 | 0.3 |
| Relative Permeability to Water,fraction | $0.75(Sw-0.2)^{2.5}$ | $0.5(0.8-Sw)^{1.5}$ |
| Relative Permeability to Oil, fraction | $0.25(Sw-0.2)^{1.5}$ | $0.5(0.8-Sw)^{2.5}$ |
| non-Darcy Flow Constant (Cb),$m^{3/2}$ | 3.20E-06 | 3.20E-06 |
| | | |
| Fluid Properties | Water | Oil |
| Viscosoty, Pa.s | 1.00E-03 | 5.00E-03 |
| Density, $kg/m^3$ | 1.00E+03 | 8.00E+02 |

Table 2 Parameter for Non-Darcy Forchheimer Displacement in a Linear Composite System

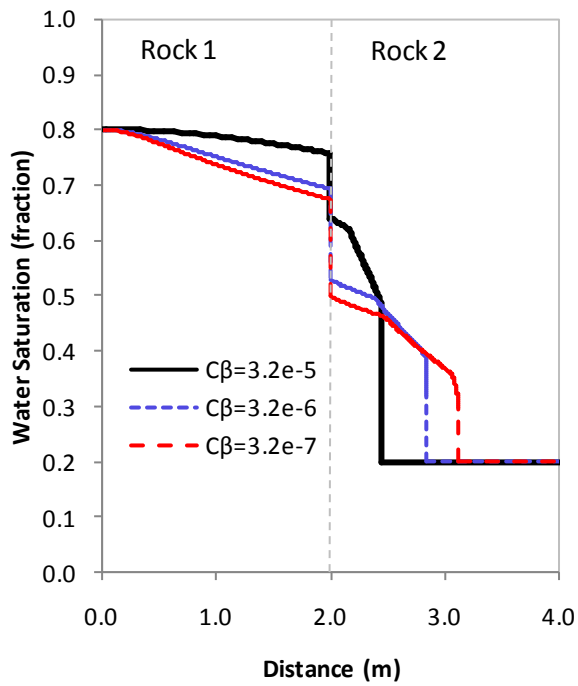


Fig. 8 Saturation Profile Comparing non-Darcy Flow constant Sensitivity

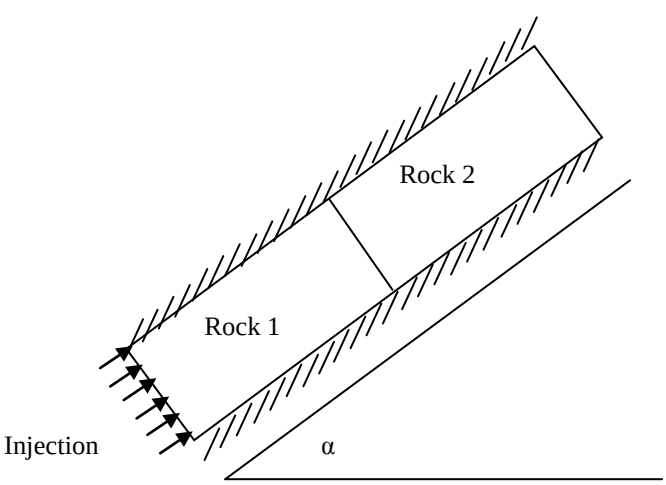


Fig. 9 Reservoir Schematic for a Linear Composite System

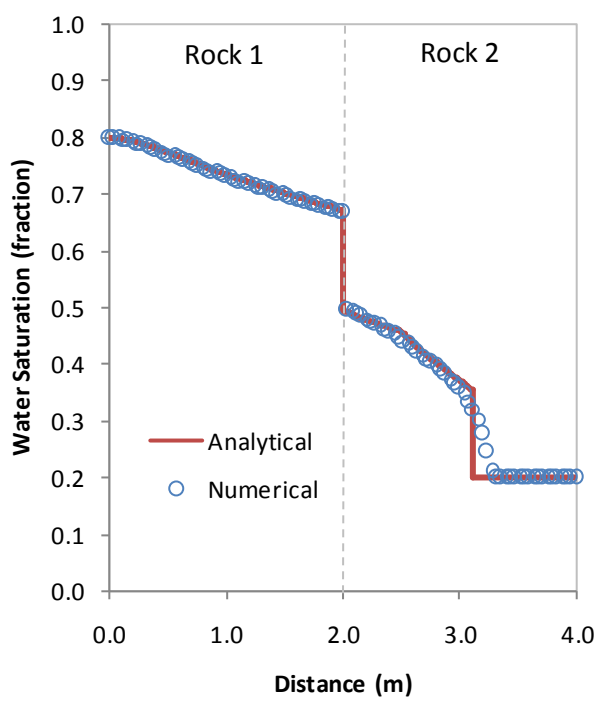


Fig. 10 Comparison of Saturation profiles between Analytical and Numerical for a Linear Composite System

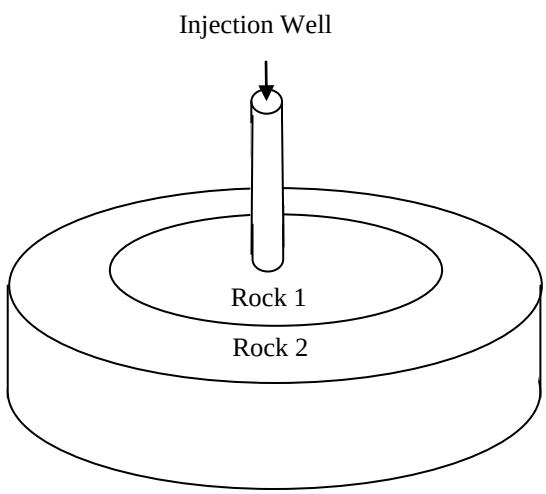


Fig. 11 Reservoir Schematic for a Radial Composite System

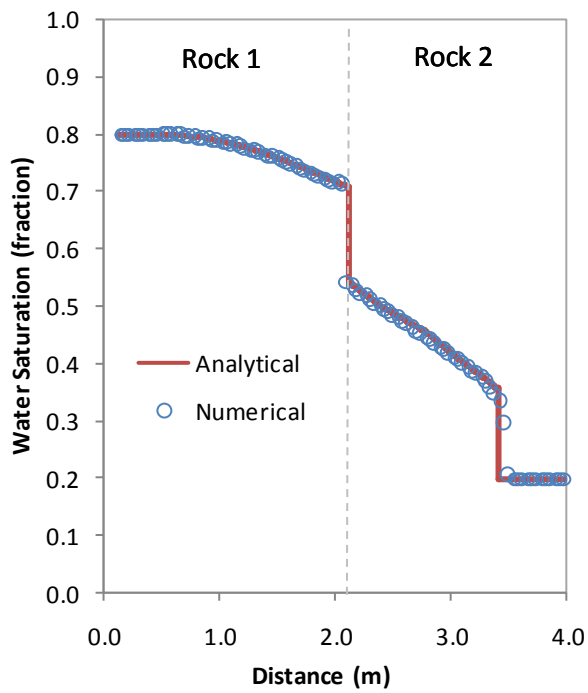


Fig. 12 Comparison of Saturation Profiles between Analytical and Numerical for a Radial Composite System

## Nomenclature

| | | |
|---|---|---|
| $A$ | = | Crossectional area, $m^2$ |
| $C_\beta$ | = | Non-Darcy flow constant, $m^{3/2}$ |
| $f_f$ | = | Fractional flow of fluid *f*, fraction |
| $h$ | = | Reservoir thickness, m |
| $k_d$ | = | Darcy permeability, $m^2$ |
| $k_r$ | = | Relative permeability ,fraction |
| $k_{mr}$ | = | Minimum permeability relative toDarcy permeability ,fraction |
| $q_i$ | = | Injection rate, $m^3/s$ |
| $r_w$ | = | Well bore radius, m |
| $r_s$ | = | Distance away from wellbore in radial system of saturation *S*, m |
| $S_f$ | = | Saturation of fluid *f*, fraction |
| $t$ | = | Given travel time after start injection, sec |
| $t^*$ | = | Travel time from start to interface of the saturation front in Rock 1, sec |
| $x_s$ | = | Distance from inlet in the x-direction of saturation *S*, m |
| $v_t$ | = | Volume metrix velocity of phase *f*, m/s |
| $v_t$ | = | Total volume metrix velocity, m/s |
| $\beta$ | = | Non-Darcyflow coefficient |
| $\Phi$ | = | Potential, Pa |
| $\tau$ | = | Characteristic length, m/10000 |
| $\rho_f$ | = | Density of fluid f,$kg/m^3$ |

| | | |
|---|---|---|
| μ | = | Viscosity, Pa.s |

## References


Aziz, K., and A. Settari, Petroleum Reservoir Simulation, Appl. Sci.,London, 1979.

Buckley, S. E., and M. C. Leverett, Mechanism of fluid displacement in sands, Trans. Am. Inst. Min. Metall. Pet. Eng., 146, 107–116, 1942.

Buckley-Leverett theory, Trans. Am. Inst. Min. Metall. Pet. Eng., 216, 271–276, 1959.

Chen, Z. X., Some invariant solutions to two-phase fluid displacement problems including capillary effect, SPE Reservoir Eng., 28, 691–700, 1988.

de Zabala, E. F., J. M. Vislocky, E. Rubin, and C. J. Radke, A chemical theory for linear alkaline flooding, Soc. Pet. Eng. J., 22, 245–258, 1982.

Evans, E. V., and R. D. Evans, Influence of an immobile or mobile saturation on non-Darcy compressible flow of real gases in propped fractures, JPT J. Pet. Technol., 40(10), 1343–1351, 1988.

Evans, R. D., C. S. Hudson, and J. E. Greenlee, The effect of an immobile liquid saturation on the non-Darcy flow coefficient in porous media, SPE Prod. Eng., 283, 331–338, 1987.

Fayers, F. J., and R. L. Perrine, Mathematical description of detergent flooding in oil reservoirs, Trans. Am. Inst. Min. Metall. Pet. Eng., 216, 277–283, 1959.

Guppy, K. H., H. Cinco-Ley, and H. J. Ramey Jr., Effects of non-Darcy flow on the constant-pressure production of fractured wells, SPEJ Soc. Pet. Eng. J., 21, 390–400, 1981.

Guppy, K. H., H. Cinco-Ley, H. J. Ramey Jr., and F. Samaniego, Non-Darcy flow in wells with finite-conductivity vertical fractures, SPEJ Soc. Pet. Eng. J., 22, 681–698, 1982.

Helfferich, F. G., Theory of multicomponent, multiphase displacement in porous media, SPEJ Soc. Pet. Eng. J., 21, 51–62, 1981.

Henderson, G. D., A. Danesh, and D. H. Tehrani, The effect of velocity and interfacial tension on relative permeability of gas condensate fluids in the wellbore region, J. Pet. Sci. Eng., 17, 256–273,1997.

Hirasaki, G. J., Application of the theory of multicomponent, multiphase displacement to three-component, two-phase surfactant flooding, SPEJ Soc. Pet. Eng. J., 21, 191–204, 1981.

Hirasaki, G. J., and G. A. Pope, Analysis of factors influencing mobility and adsorption in the flow of polymer solution through porous media, Soc. Pet. Eng. J., 14, 337–346, 1974.

Karakas, N., S. Saneie, and Y. Yortsos, Displacement of a viscous oil by the combined injection of hot water and chemical additive, SPE Reservoir Eng., 1, 391–402, 1986.

Katz, D. L., and R. L. Lee, Natural Gas Engineering, Production and Storage, McGraw-Hill, New York, 1990. Larson, R. G., and G. J. Hirasaki, Analysis of the physical mechanisms in surfactant flooding, Soc. Pet. Eng. J., 18, 42–58, 1978.

Lai, B., Miskimins, J. L., and Wu, Y. S., Non-Darcy Porous Media Flow According to the Barree and Conway Model: Laboratory and Numerical Modeling Studies, SPE 122611, 2009.

Larson, R. G., H. T. Davis, and L. E. Scriven, Elementary mechanisms of oil recovery by chemical methods, JPT J. Pet. Technol., 34(2), 243–258, 1982.

Lee, R. L., R. W. Logan, and M. R. Tek, Effects of turbulence on transient flow of real gas through porous media, SPE Form. Eval., 108–120, 1987.

Liu, X., F. Civan, and R. D. Evans, Correlations of the non-Darcy flow coefficient, J. Can. Pet. Technol., 34(10), 50–54, 1995.

McWhorter, D. B., and D. K. Sunada, Exact integral solutions for two-phase flow, Water Resour. Res., 26(3), 399–413, 1990.

Wu, Y. S., K. Pruess, and Z. X. Chen, Buckley-Leverett flow in composite porous media, SPE Adv. Technol. Ser., 1(2), 36–39, 1993.

Wu, Y. S., Non-Darcy displacement of immiscible fluids in porous media, Water Resources Research. Vol. 37, NO. 12, 2943–2950, 2001.
Wu, Y. S., K. Pruess, and P. A. Witherspoon, Displacement of a Newtonian fluid by a non-Newtonian fluid in a porous medium,Transp. Porous Media, 6, 115–142, 1991.
Wu, Y. S., K. Pruess, and P. A. Witherspoon, Flow and displacement of Bingham non-Newtonian fluids in porous media, SPE Reservoir Eng., 7, 369–376, 1992.
Wu, Y.S., Lai, B. T. et al. Simulation of multiphase non-Darcy flow in porous and fractured media, SPE 122612, 2009.

## Appendix A Example Calculation for a Linear Composite System

This example is selected to demonstrate the calculation method for a linear composite system. The approach is also applied to a radial composite, only minimum modification is required. It is assumed that fractional flow curve is known using rock property is given in Table 1.

From the fractional flow curves, we can calculate the shock front saturation of Rock 1 and Rock 2 using Welge's graphical method, see Fig. A-1. In this example, it is indicated that $S_{f1} > S_{f2}$. Note that there is another case ($S_{f1} < S_{f2}$). Here, the case ($S_{f,1} > S_{f,2}$) is the most interested. Saturation of Rock 1 at interface ($S^-$) is calculated by

$$\left(\frac{\partial f_w}{\partial S_w}\right)_{S^-} = \frac{\phi_1 A L_1}{q_i t} \tag{A-1}$$

where, $L_1$ is length of Rock 1 or interface location

From continuity condition between interface, Equation (19), we can calculated the water saturation at the interface of Rock 2 ($S^+$) . For this example, water saturation profile in Rock 2 has a discontinuity because when the shock front in Rock 1 reaches interface, the front saturation ($S_{f1}$) has the corresponding apparent saturation in domain 2 ($S^*$) higher than the shock front saturation ($S_{f2}$). Consequently, only the shock front saturation travels with the fastest speed whereas saturation higher than that ($S_{f2}<S<S^*$) travels with gradually lower speed. When time goes by, water saturation which higher than S* reaches interface and starts travel with even lower speed. As this subsequent saturation reach the interface after S*, thus, travel time in Rock 2 is less than that of saturation of S*. As the results discontinuity appears. Water saturation profile can be calculated as follows

(1) The water saturation profile in Rock 1($1-S_{or}<S_w<S^-$) is calculated by the following equation:

$$x_{s1} = \frac{q_i t}{\phi_1 A}\left(\frac{\partial f_w}{\partial S_w}\right)_{S_1} \qquad \left(S_1 > S_1^-\right) \tag{A-2}$$

(2) The water saturation profile in Rock 2 is divided in to three parts a) the shock front ($S<S_{f2}$), b) ($S_{f2}<S<S^*$), and C) ($S^*<S<S^-$) each region is calculated as follows

a) The shock front location ($S<S_{f2}$),

$$x_{s_{f2}} = L_1 + \frac{q_i(t-t^*)}{\phi_1 A}\left(\frac{\partial f_w}{\partial S_w}\right)_{S_{f2}} \tag{A-3}$$

Where $t^*$ is the time of shock front saturation $S_{f1}$ arriving at the interface and can be computed by the following equation:

$$t^* = \frac{\phi_1 A L_1}{q_i\left(\frac{\partial f_w}{\partial s_w}\right)_{s_{f1}}} \tag{A-4}$$

b) ($S_{f2}<S<S^*$), as these saturation reaches Rock 2 as the same time as the shock front, we can use the same travel time as the shock front

$$x_{s_2} = L_1 + \frac{q_i(t-t^*)}{\phi_1 A}\left(\frac{\partial f_w}{\partial S_w}\right)_{S_2} \qquad \left(S_{f2} < S_2 < S^*\right) \tag{A-5}$$

c) and ($S^*<S<S^-$), these saturation reaches Rock 2 later than that of previous saturations, as such the travel is in Rock 2 is shorter

$$x_{s_2} = L_1 + \frac{q_i(t-t_2)}{\phi_1 A}\left(\frac{\partial f_w}{\partial S_w}\right)_{S_2} \qquad \left(S^* < S_2 < S^+\right) \tag{A-6}$$

Where $t_2$ is the time of the apparent saturation in Rock 1 of the selected $S_2$ arriving at the interface and can be computed by the following equation:

$$t_2 = \frac{\phi_1 A L_1}{q_i\left(\frac{\partial f_w}{\partial s_w}\right)_{s_{21}}} \tag{A-7}$$

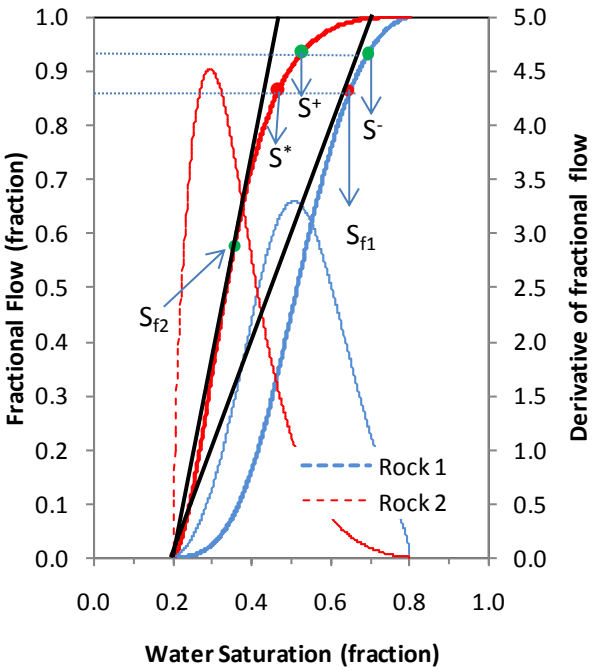


Fig. A-1 Fractional Flow and Its Derivative

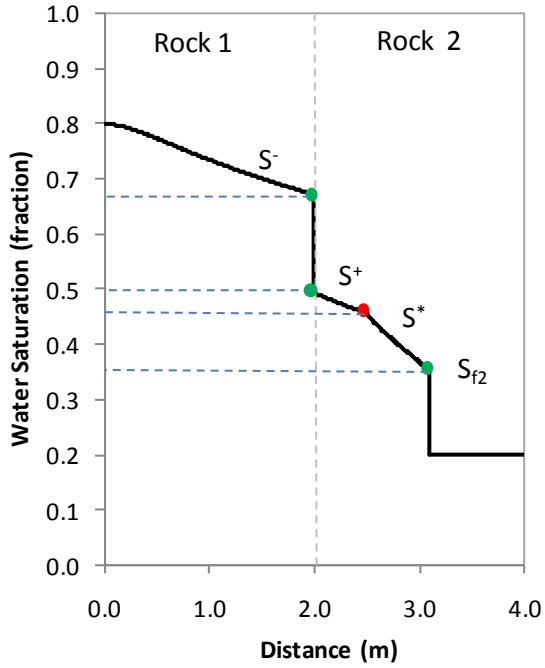


Fig. A-2 Saturation Profile